 FDMP, vol.3, no.4, pp.329-337, 2007

Axially Running Wave in Liquid Bridge

D.E. Melnikov[1] **and V.M. Shevtsova**[2]

Abstract: Thermocapillary convection in a long vertical liquid column (called liquid bridge) subjected to heating from above is considered for a three-dimensional Boussinesq fluid. The problem is solved numerically via finite-volume method. Full system of three dimensional Navier-Stokes equations coupled with the energy equation is solved for an incompressible fluid. Instability sets in through a wave propagating in axial direction with zero azimuthal wave number, which is a unique stable solution over a wide range of supercritical heating. Further increasing the applied temperature difference results in bifurcation of a second wave traveling azimuthally with a slightly higher frequency. The two waves co-exist within a certain range of the supercritical parameter and finally the axially running one gets suppressed while the azimuthal gets stronger.

Keyword: Thermocapillary convection, hydrothermal wave, liquid bridge, instability, CFD.

1 Introduction

Study of thermocapillary convective flow in liquid bridge has attracted much of attention due to its relation to technological process of crystal growth by floating zone method. Liquid bridge, a configuration where liquid volume is held between two differentially heated horizontal flat disks, is a model representing a half of the floating zone. With the aim of this simplified geometry, which well incorporates some of the complexities of full zone, one aims at understanding the transport processes involved in the crystal growth by this method. Surface tension gradient along the free surface drives the liquid from the hotter toward the colder endwall resulting in a return flow. This flow is two-dimensional at relatively small imposed temperature differences ΔT. At a certain value of the temperature difference (critical value ΔT_{cr}), the two-dimensional stationary thermo convective flow undergoes transition to a three-dimensional either stationary or oscillatory regime along with pattern formation. Both ΔT_{cr} and type of the supercritical flow are defined by parameters of the system (Prandtl number, temperature difference, gravity, liquid volume, ambient conditions etc.). In high Pr liquid bridges (Pr larger than ≈ 0.02) hydrothermal instability is oscillatory and starts as a result of a supercritical Hopf bifurcation as either traveling or standing waves [Wanschura, Shevtsova, Kuhlmann, and Rath (1995); Frank and Schwabe (1997); Shevtsova, Melnikov, and Legros (2001)].

Study of the onset of the oscillatory convection in liquid bridge was extensively carried out both theoretically [see e.g. Lappa (2005); Gelfgat, Rubinov, Bar-Yoseph, and Solan (2005); Lan and Yeh (2005)] and experimentally [for example, Shevtsova, Mojahed, and Legros (1999); Schwabe (2005); Kamotani, Matsumoto, and Yoda (2007)]. The attention was paid to both the development of the oscillatory regime and spatial organization of the thermocapillary flow. The critical temperature difference, or suitably defined critical *thermocapillary* Reynolds number $Re_{cr} \propto \Delta T_{cr}$, was calculated and measured for different liquids and geometries.

There are some correlations suggested for description of the spatial structure of the flow in the bulk. To characterize the spatial symmetry of the flow, a concept of azimuthal wave number m was suggested. In the supercritical regime, the field of temperature deviations from the azimuthally

[1] e-mail:dmelniko@ulb.ac.be, Free University of Brussels (ULB), Brussels, Belgium.

[2] e-mail: vshev@ulb.ac.be, Free University of Brussels (ULB), Brussels, Belgium.

uniform field (disturbances) have a structure of a set of hot and of the same number of cold patterns. Consequently, the number of the hot (or cold) patterns is equal to m. The wave number at the threshold of instability is called critical mode. The flow structure in liquid bridge in the supercritical parameters' region is very similar to that observed for a flow in infinite high-Pr liquid column ($m = 1$ at $\Gamma = \infty$) [Xu and Davis (1984)]. However, the system's spatial limitation changes the critical mode (for instance at $\Gamma = 1, Gr = 0$, it is not $m = 1$ as it should be in an infinitely long liquid bridge according to the theory, but $m = 2$ [Shevtsova, Melnikov, and Legros (2001)]). The first empirical correlation for the determination of the critical mode, $m \approx 2.2/\Gamma$, has been suggested in [Preisser, Schwabe, and Scharmann (1983)] analyzing the experimental data for a fluid with $Pr = 8.9$. In the above expressions Γ stands for aspect ratio (height to radius ratio).

A slightly different correlation, $m \approx 2.0/\Gamma$, has been obtained numerically for $Pr < 7$ assuming pure Marangoni convection without buoyancy force [Leypoldt, Kuhlmann, and Rath (2000)]. The relation $m \approx 2.0/\Gamma$ does not hold if $Pr \geq 30$. It was experimentally demonstrated for aspect ratios close to one for different silicone oils with $Pr \geq 30$ that $m = 1$ at the threshold of instability [Carotenuto, Castagnolo, Albanese, and Monti (1998); Shevtsova, Mojahed, and Legros (1999); Muehlner, Schatz, Petrov, McCormic, Swift, and Swinney (1997)]. The three-dimensional numerical calculations [Shevtsova, Melnikov, and Legros (2001)] have also confirmed that this empirical relation is not valid for $Pr = 35$. Further increasing the temperature difference gives birth to higher wave numbers ($m > 1$), which can either co-exist with [Melnikov, Shevtsova, and Legros (2004)] or develop independently of the critical mode [Shevtsova, Melnikov, and Legros (2003)].

Both the above-mentioned relations and the result of the theoretical study rule out any possibility of existing a solution with $m = 0$ mode in geometries with $\Gamma < 2$. It is worth mentioning however that existence of stable solution in a form of axially running wave was predicted for infinitely large non-isothermal liquid columns with $Pr > 50$ [Xu and Davis (1984)]. Nevertheless, there was an experimental evidence of occurrence of the $m = 0$ mode [Velten, Schwabe, and Scharmann (1991)]. Investigating the oscillation modes over wide ranges of aspect ratios and ΔT by using three thermocouples positioned at an angle of 45 degrees from one another, Velten and co-workers identified them via the phase shifts between the thermocouple signals. They found that in some cases phase shifts did not occur, while in some other cases phase shifts continuously changed with increasing the temperature difference. This occurrence was explained by the existence of axially running waves. Zero phase shifts were explained by the axially running waves with symmetric wave fronts while the continuously changing were justified by the axially running waves but with deformed wave fronts.

In ground experiments on a 10 cSt silicone oil liquid bridge with aspect ratio 1.2, Shevtsova and coauthors [Shevtsova, Mojahed, Melnikov, and Legros (2003)] have reported on an oscillatory regime of the flow characterized by $m = 0$ critical mode. This solution existed only in a narrow range of values of the temperature difference just after the onset of oscillations, and it was rapidly suppressed by $m = 1$ mode with a lower frequency while increasing ΔT. The $m = 0$ regime of the flow is an azimuthally uniform oscillatory solution. Thus, thermocouples placed at the same vertical position would record in-phase temperature oscillations.

In the present work, a three-dimensional full Navier-Stokes equations were solved numerically for a liquid bridge of $\Gamma = 1.8$ aspect ratio formed by 1 cSt silicone oil with $Pr = 14$. We show that instability occurs first at zero azimuthal wave number. It begins as oscillatory $m = 0$ mode, which remains stable up to $\approx 1.5\ \Delta T_{cr}$ and gets dominated by $m = 1$ traveling wave at higher Re. Within the range of parameters where both wave numbers co-exist, the system's dynamics become very complicated resulting from complex nonlinear interactions between them. Their understanding, therefore, demands a profound analysis by decomposing the complex flow into simple waves and quantifying the effect of each of them.

2 Description of model

A cylindrical liquid bridge of radius R and of height d is sketched in Fig. 1. The temperatures T_{hot} and T_{cold} ($T_{hot} > T_{cold}$) are prescribed at the upper and lower walls respectively, $\Delta T = T_{hot} - T_{cold}$. Density ρ, surface tension σ, and kinematic viscosity ν of the liquid are taken as linear functions of the temperature:

$$\rho = \rho(T_0) - \rho_o\beta(T - T_0), \quad \beta = -\rho_0^{-1}\frac{\partial\rho}{\partial T},$$
$$\sigma(T) = \sigma(T_0) - \sigma_T(T - T_0), \quad \sigma_T = -\frac{\partial\sigma}{\partial T},$$
$$\nu(T) = \nu(T_0) + \nu_T(T - T_0), \quad \nu_T = \frac{\partial\nu}{\partial T}.$$

where $T_0 = T_{cold}$.

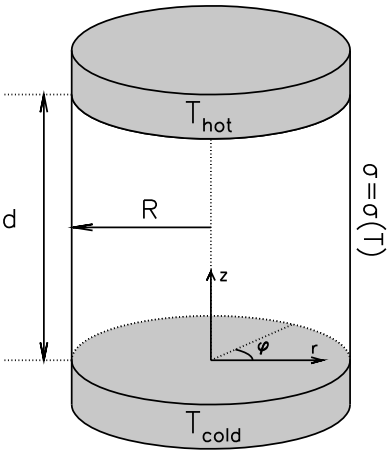

Figure 1: Liquid bridge

The phenomena to be considered are described by a system of three-dimensional Navier-Stokes equation with a buoyancy force term, the incompressibility constraint and the energy equation:

$$\frac{\partial\mathbf{V}}{\partial t} + (\mathbf{V}\cdot\nabla)\mathbf{V} = -\nabla P + 2R_\nu\mathbf{S}\times\nabla(\Theta + z) + (1 + R_\nu(\Theta + z))\triangle\mathbf{V} + \vec{e}_z Gr(\Theta + z), \quad (1)$$
$$\nabla\cdot\mathbf{V} = 0, \quad (2)$$
$$\frac{\partial\Theta}{\partial t} + \mathbf{V}\cdot\nabla\Theta = -V_z + \frac{1}{Pr}\triangle\Theta, \quad (3)$$

where $\mathbf{V} = (V_r, V_\varphi, V_z)$ is velocity, $\Theta = (T - T_0)/\Delta T - z = \Theta_0 - z$ is temperature and t is time. The strain rate tensor $\mathbf{S} = \{S_{ij}\} = (1/2)(\partial V_i/\partial x_k + \partial V_k/\partial x_i)$.

The dimensionless parameters in eqs.(1)-(3) are Prandtl, Grashof, "thermocapillary" Reynolds numbers and viscosity contrast:

$$Pr = \frac{\nu(T_0)}{k}, \qquad Gr = \frac{g\beta\Delta T d^3}{\nu(T_0)^2},$$
$$Re = \frac{\sigma_T\Delta T d}{\rho(T_0)\nu(T_0)^2}, \quad R_\nu = \frac{\nu_T\Delta T}{\nu(T_0)}.$$

where k, β and g are thermal diffusivity, thermal expansion coefficient and acceleration due to gravity.

A following set of boundary conditions is prescribed. On the rigid thermally conducting boundaries ($z = 0, 1$) there are no slip, impermeability and fixed temperature conditions:

$$\mathbf{V}(r,\varphi,z=0,t) = \mathbf{V}(r,\varphi,z=1,t) = 0.$$
$$\Theta(r,\varphi,z=0,t) = \Theta(r,\varphi,z=1,t) = 0.$$

On the adiabatic free surface ($r = 1$):

$$V_r = 0,$$
$$2[1 + R_\nu(\Theta + z)]\mathbf{S}\cdot\mathbf{e_r} + Re\left(\mathbf{e_z}\partial_z + \mathbf{e}_\phi\frac{1}{r}\partial_\phi\right)(\Theta + z) = 0,$$
$$\partial\Theta/\partial r = 0.$$

The three-dimensional governing equations are solved on a $[N_r, N_\varphi, N_z] = [24\times16\times30]$ mesh non-uniform both in the radial and axial directions with minimum intervals near the interface (0.025) and at the cold wall (0.02). Also, a test was performed on a $[N_r, N_\varphi, N_z] = [48\times16\times40]$ mesh for a slightly supercritical value $Re = 1155$ to verify that the solution is correct. The $[24\times16\times30]$ grid was proved to be sufficient in case of a liquid with $Pr = 18$ (see [Melnikov, Shevtsova, and Legros (2004)]). Both description of numerical method and code validation could be found in the same paper.

In the present study we consider a liquid bridge of $R = 2.5$ *mm* radius and $d = 4.5$ *mm* height (thus, with aspect ratio $\Gamma = d/R = 1.8$) formed by 1 cSt silicone oil of $Pr = 14$. The control parameter

for the system is the applied temperature difference, ΔT, changing it entrains variations of Re, Gr and R_ν. Re is varied between 0 and 1250 and the Grashof number and the relative viscosity contrast are changing together with the Reynolds number according to:

$$Gr/Re = 3.11,\ R_\nu/Re = 1.46 \cdot 10^{-5}.$$

The analyzed below solutions exhibit, that above the threshold of instability, the flow organization includes combination of azimuthal and longitudinal waves. In general, the oscillatory motion consists of two pairs of counter propagating waves both in the azimuthal φ and axial z directions:

$$\begin{aligned}
&(\mathbf{V},\Theta)(r,\varphi,z,t) = (\overline{\mathbf{V}},\overline{\Theta})(r,z)\\
&+(\hat{\mathbf{V}}_{left},\hat{\Theta}_{left})exp(i[m\varphi-(i\lambda_1+\omega_1)t])\\
&+(\hat{\mathbf{V}}_{right},\hat{\Theta}_{right})exp(i[-m\varphi-(i\lambda_1+\omega_1)t+g(r,z)])\\
&+(\hat{\mathbf{V}}_{up},\hat{\Theta}_{up})exp(i[nz-(i\lambda_2+\omega_2 t)])\\
&+(\hat{\mathbf{V}}_{down},\hat{\Theta}_{down})exp(i[-nz-(i\lambda_2+\omega_2 t)])+c.c.
\end{aligned}$$

where $\mathbf{k} = (0;m;n)$ and ω_1, ω_2 are wave vector and frequencies of azimuthal and axial waves, respectively; λ_1, λ_2 are growth rates; m is earlier introduced azimuthal wave number. The function $g(r,z)$ is the phase describing the inclination of the wave with respect to the vertical axis. $\overline{\mathbf{V}}, \overline{\Theta}$ denote velocity and temperature fields of two-dimensional basic state, and the subscripts $left, right, up, down$ stand for amplitudes of the waves propagating counterclockwise, clockwise, up and down stream. Depending upon the ratios between amplitude of two counter propagating waves, one can observe either standing (equal amplitudes) or traveling (different amplitudes) waves.

For examined parameters different flow organizations are possible:

• $m = 0$, $n \neq 0$. Axially spreading (longitudinal) wave.

• $m \neq 0$, $n = 0$. Azimuthal standing or traveling wave.

• $m \neq 0$, $n \neq 0$. Mixed wave, the wave vector forms some angle with respect to the axial direction.

3 Results

Before proceeding further with our discussion of results of simulations, let's briefly reflect on some of the properties of the three mentioned above solutions. One of the integral quantities of the flow past bifurcation is net azimuthal flow. A flow in the azimuthal direction is caused by a non-uniformity of the temperature field in this direction. The net azimuthal flow is an integral of the mean azimuthal velocity over the volume

$$\begin{aligned}
&\overline{V}_{mean}(r,z,t) = \frac{1}{2\pi}\int_0^{2\pi} V_\varphi(r,z,\varphi,t)d\varphi,\\
&\Phi = \int \overline{V}_{mean}(r,z,t)rdrdz. \qquad (4)
\end{aligned}$$

It provides information about the nonlinear characteristics of the flow organization allowing to say if the wave is standing ($\Phi = 0$) or traveling ($\Phi \neq 0$) [Shevtsova, Melnikov, and Legros (2001)].

The net azimuthal flow is non-zero only in case of traveling azimuthal wave, for which $\hat{\mathbf{V}}_{left} \neq \hat{\mathbf{V}}_{right}$. If the wave is standing then $\Phi = 0$. In case of $m = 0$, there is an absolute uniformity in the φ direction. Thus, longitudinal wave is a motion with $V_\varphi = 0$ ($\Phi = 0$).

To distinguish between axially running $m = 0$ and azimuthal standing waves one needs to analyze local temperature oscillations. Similar to experiment, we monitored temperature field locally at four locations. Since longitudinal wave is azimuthally uniform, the temperature signals recorded at two arbitrary points with the same radial and axial coordinates but shifted azimuthally on some angle α should coincide regardless the angle. In turn, the temperature signals do not coincide in case of azimuthal wave unless $\alpha \neq 2\pi/m$.

Let's now pass to discussion of findings of the work.

3.1 Axially running wave (ARW), m = 0

A wave spreading in axial direction bifurcates directly from the two-dimensional subcritical flow at the critical value of the Reynolds number $Re_{cr} = 990$. Temperature time-series recorded

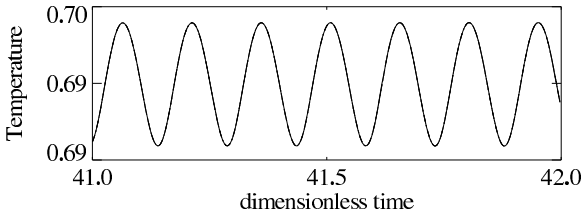

Figure 2: Axially running wave when $Re = 1050$. Temperature time-series monitored at four equidistant locations at $(r = 1, z = 0.9)$.

at any points with the same radius and height *absolutely* coincide (Fig. 2). This is a feature of the solution with $m = 0$, i.e. azimuthal uniformity of the variables. Analysis shows that the wave is more intensive closer to the interface, where the temperature oscillates with a larger amplitude. The closer to the symmetry axis $r = 0$, the smaller the amplitude of the temperature oscillations is.

The liquid bridge is known to be particularly sensitive to initial state in the supercritical area (see e.g. [Melnikov, Shevtsova, and Legros (2005)]). To check if the longitudinal wave is really a unique and stable solution at the threshold of instability, three different initial guesses were taken for the simulations: two-dimensional (2D) and three-dimensional (3D) both azimuthally standing and traveling waves. Within the appropriate range of the Reynolds numbers (between 990 and 1155) any initial state has always been converging to the same final solution, i.e. longitudinal hydrothermal wave with $m = 0$.

To visualize the axially running wave slightly above the bifurcation point at $Re = 1050$, Fig. 3 is suggested. It shows time-series of the mean temperature $< \Theta >$ (eq. 5) at different heights. The mean temperature is an averaged in a cross-section field:

$$< \Theta > (z,t) = \frac{1}{2\pi} \int_0^1 \int_0^{2\pi} \Theta_0(r, \varphi, z, t) r dr d\varphi. \quad (5)$$

Amplitude of the $< \Theta >$ oscillations is not constant, it attains its maximum values near the cold and the hot walls and is of one order of magnitude smaller in the mid-plane region (Fig. 3, 4). Contrary to our results, in a set of experiments carried

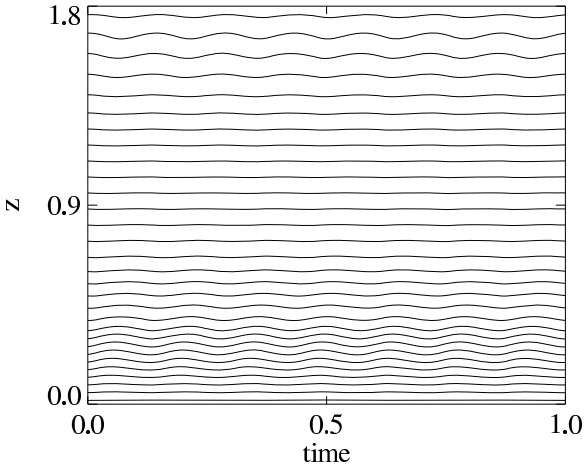

Figure 3: Axially running wave at $Re = 1050$. Oscillations of mean temperature $< \Theta >$ recorded at different heights.

out on a $Pr = 30$ and much longer liquid bridge of $\Gamma = 5$ under $0 - g$ (see Fig.8 in [Schwabe (2005)]), the temperature oscillations are of the largest amplitude in the mid-plane area and are very weak near the walls, especially near the hot end-wall.

The axially spreading wave is non-sinusoidal (Fig. 4) with its amplitude equal zero at the rigid walls. The oscillations of $< \Theta >$ near the hot and the cold walls are in counter phase, i.e. when a hot pattern is formed in the upper part there is a cold one bellow. The length of periodicity of the *ARW* could be estimated as a double distance between minima and maxima of $< \Theta >$. Our estimations show that it is approximately 50% larger compared to the height of the liquid bridge, $\lambda = 1.5d$. Moreover, one might think that the axial wave is standing but indeed it is traveling as there are no points along the medium which appear to be standing still (nodes) - a typical feature of any standing wave. In Fig. 4 one can see $< \Theta >$ profiles for six consecutive equidistant in time moments showing that the node is not standing. Interestingly, there are time instances when the mean temperature profile along z has two nodes (dash-dot curve on Fig. 4) and $< \Theta >$ has the same sign both near the cold and hot walls. Thus, at any time the mean temperature always deviates from zero.

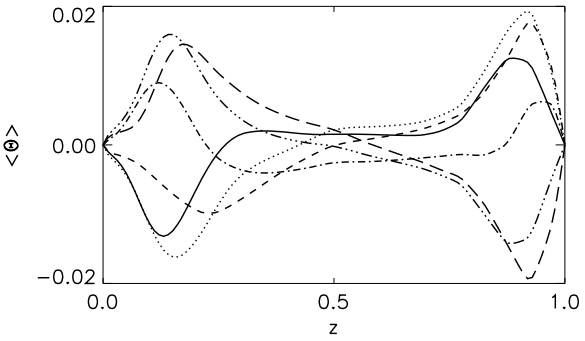

Figure 4: Snapshots of $< \Theta >$ profile along the liquid bridge's length at 6 consecutive times. Profiles are made for $Re = 1050$. Consequence of the frames is the following: 1 - solid, 2- dotted, 3 - dashed, 4 - dash-dot, 5 - dash-dot-dot-dot, 6 - long-dashes lines.

Figure 5: Frequencies of axially running (solid line) and azimuthally traveling (dashed line) waves. Hydrothermal wave running in axial direction described by $m = 0$ wave number bifurcated directly from two-dimensional basic state 2D.

Fig. 4 suggests that the node (the point where the curves cross $< \Theta >= 0$) is moving up stream (the frames are presented in the following order: the first frame is plotted by the solid line, followed by the dotted, dashed and then by the dash-dot,dash-dot-dot-dot, long-dashes lines). The node and the axially running wave are traveling in the same direction, i.e. the longitudinal wave originates near the cold wall.

Knowing the frequency ω_2, one can estimate speed of propagation of the *ARW* assuming that the latter is harmonic. The frequencies of the temperature oscillations recorded at $(r, \varphi, z) = (1.0, 0, 0.5)$ point are plotted on Fig. 5 for the whole studied range of the Reynolds numbers. Solid line represents the frequencies of the axial wave. To get the dimensional value of the frequency, one should multiply the corresponding value from Fig. 5 by $0.008 sec^{-1}$. Thus, estimations give the velocity of the spreading of the axially running wave $V_{ARW} = 0.008 \cdot 1.5 d \cdot \omega_2 \approx 2.30\ mm/s$ at $Re = 1000$ and increasing up to $2.61\ mm/s$ when $Re = 1230$.

The frequency of the axially running wave grows almost linearly with increase of the Reynolds number (Fig. 5):

$$\omega_2 = 42.47 + 0.022 Re.$$

Analysis shows that the amplitude of the $m = 0$ mode also increases. Thus the wave motion transports more energy when the applied ΔT is larger. The amplitude of the $< \Theta >$ oscillations is slightly larger near the hot wall (Fig. 4), i.e. the hydrothermal wave gets amplified while moving up stream crossing the region of higher temperature.

3.2 Azimuthal wave (HTW), m = 1

At about $Re = 1155$ a second solution appears. A hydrothermal wave (HTW) running in azimuthal direction appears at the second bifurcation. Analysis shows that it is described by $m = 1$ wave number (one hot and one cold rotating patterns seen in the temperature disturbances field). This second solution has a slightly higher frequency ω_1 compared to the one of the axial wave ω_2 (Fig. 5) which does not vary much within $1155 < Re < 1250$ (dashed line on Fig. 5). The second independent solution with $m = 1$ starts to manifest itself in splitting the temperature oscillations recorded at different locations. The temperature time-series in two points with the same radial and axial co-ordinates do not completely coincide as before at $Re < 1155$ (compare Figs. 6 and 2). This slight splitting is a result of propagation of the second wave in the azimuthal direction, which at $Re = 1200$ is still relatively weak compared to the $m = 0$ developed oscillations.

As was already mentioned in the introduction, ground-based experimental observations revealed that the frequency of the azimuthally traveling wave was lower than the one of the axially run-

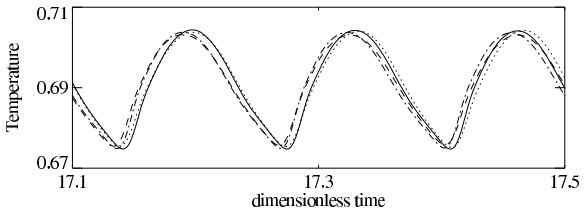

Figure 6: Axial and azimuthal waves co-existing at $Re = 1200$. Temperature time-series monitored at four equidistant locations at $(r = 1, z = 0.9)$.

ning waves [Shevtsova, Mojahed, Melnikov, and Legros (2003)]. Direct comparison with the experiment could not be done since the calculations were performed for different liquid and aspect ratio. However, for the considered system the calculations led to an opposite situation although they coincide as for the consequence of the bifurcating solutions.

Reconstructed $< \Theta >$ time-series for the azimuthally traveling wave do not show any oscillations, which we observed in the case of longitudinal wave (see Fig. 3). At any two opposite points in a horizontal cross-section (r, φ, z) and $(r, \pi + \varphi, z)$ the temperature disturbances have the same absolute values but different signs and thus, they will give zero input to $< \Theta >$.

The azimuthally running and the hydrothermal waves co-exist between $Re = 1155$ and 1232, a so-called mixed mode solution when the wave vector $\mathbf{k} = (0; m; n)$ has both nonzero wave vector components. The stable mixed modes have already been observed in some studies on liquid bridge [Melnikov, Shevtsova, and Legros (2004)] where two azimuthally traveling waves with $m =$ 1 and 2 were spreading in liquid bridge simultaneously. The mixed mode was not observed in the experiment [Shevtsova, Mojahed, Melnikov, and Legros (2003)]. The two waves described by $m = 0$ and 1 co-existed for extremely short interval of ΔT.

Fig. 7 represents how the net azimuthal flow (eq. 4) changes versus the Reynolds number. The bifurcation points are:

• Onset of instability at $Re = 990$ in form of axially running wave (it is not seen as Φ keeps zero value).

• origin of the HTW at about $Re = 1155$ where Φ deviates from zero.

• the third bifurcation at $Re \approx 1232$ where the mode $m = 1$ becomes dominant.

At $Re = 1155$, the point where the azimuthally traveling wave originates, the net azimuthal flow starts growing. This is an expected result, given the fact that for any azimuthally traveling wave $\Phi \neq 0$.

At $Re > 1232$ only pure $m = 1$ azimuthally traveling wave pattern exists. The oscillations of temperature recorded at the four equidistant locations are $\pi/2$ phase shifted. They are of the same amplitude at all the four points. At $Re \approx 1232$, the point where the axial wave disappears, the net azimuthal flow's growth rate increases resulting from redistribution of energy available for hydro thermal waves propagation. Its growth rate became higher due to the fact that no more energy is taken for the growing $m = 0$ mode.

Similar effect, which we called deviation from regular branch when studied transition to chaotic flow in a liquid bridge with $Pr = 4$ [Shevtsova, Melnikov, and Legros (2003)], is caused by redistribution of the energy among modes. We observed that within a region where the solution became quasi-periodic or aperiodic Φ got reduced and thus deviated from smooth regular curve. We suggested an explanation that it happened due to the energy transfer from the mean flow into the growing disturbances.

This mechanism could work for explanation of the third bifurcation in the considered problem. Since the axial wave vanishes and thus all the energy goes to the azimuthally running motion, whose intensity grows leading to increasing the net azimuthal flow.

Interestingly, it seems that the $m = 0$ axial wave exists only in some narrow range of parameters and under specific conditions. Changing gravity, for example, results in changing the wave vector. Under microgravity conditions, a $m = 1$ traveling wave bifurcates from the 2D state. It permits to suggest that a simultaneous effect of several factors (aspect ratio and ratio between buoyancy

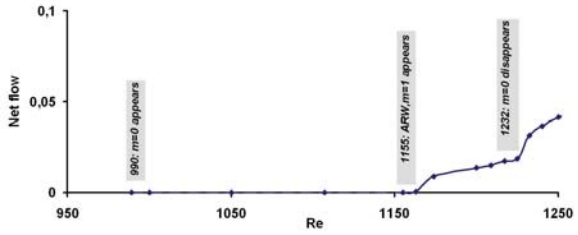

Figure 7: Net azimuthal flow allowing to trace two bifurcations passed by the flow at $Re = 1155$ and $Re = 1232$. Instability begins at $Re = 990$ as $m = 0$ axial wave with zero net azimuthal flow.

and thermocapillary force Gr/Re) may generate a longitudinal wave motion. The system should be long enough for the axially running wave to have room to get established, but not too long to avoid strong prevailing of one of the two mentioned above forces. To find conditions when the axially running wave is stable demands a future study which will involve variations of both gravity and of the length of the liquid bridge.

4 Conclusions

In this paper, a convective flow caused by coupled thermocapillary forces and buoyancy is studied via direct computer simulations in a high Prandtl number liquid ($Pr = 14$). In the considered long non-isothermal liquid column of 2.5 *cm* radius and 4.5 *cm* length under normal gravity conditions, instability starts as a pure $m = 0$ axially running wave that does not break the azimuthal symmetry of the basic two-dimensional state. This solution is a new finding, which has never been predicted for $Pr < 50$. Calculations performed on different computational grids prove that this is a unique and stable solution near the threshold of instability. The axially running wave originates in the near cold wall region and travels up stream with an estimated velocity varied between 2.30 and 2.61 mm/s depending on the Reynolds number. Increasing Re increases the wave velocity.

Even if the instability starts as a $m = 0$ axially running wave, an azimuthally traveling one always appears at a higher value of the Reynolds number. There is a range of Re where the two waves co-exist and finally the growing azimuthal oscillatory motion "overpowers" the longitudinal one and the latter disappears. This phenomenon is clearly seen on the net azimuthal flow curve when its growth rate noticeably increases compared to the mixed $m = 0 + 1$ solution.

References

Carotenuto, L.; Castagnolo, D.; Albanese, C.; Monti, R. (1998): Instability of thermocapillary convection in liquid bridges. *Phys. Fluids*, vol. 10, pp. 555 – 565.

Frank, S.; Schwabe, D. (1997): Temporal and spatial elements of thermocapillary convection in a liquid zone. *Experiments in Fluids*, vol. 23, pp. 234 – 251.

Gelfgat, A. Y.; Rubinov, A.; Bar-Yoseph, P. Z.; Solan, A. (2005): On the Three-Dimensional Instability of Thermocapillary Convection in Arbitrarily Heated Floating Zones in Microgravity Environment. *FDMP: Fluid Dynamics & Materials Processing*, vol. 1, no. 1, pp. 21 – 32.

Kamotani, Y.; Matsumoto, S.; Yoda, S. (2007): Recent Developments in Oscillatory Marangoni Convection. *FDMP: Fluid Dynamics & Materials Processing*, vol. 3, no. 2, pp. 147 – 160.

Lan, C. W.; Yeh, B. C. (2005): Effects of Rotation on Heat Flow, Segregation, and Zone Shape in a Small-scale Floating-zone Silicon Growth under Axial and Transversal Magnetic Fields. *FDMP: Fluid Dynamics & Materials Processing*, vol. 1, no. 1, pp. 33 – 44.

Lappa, M. (2005): Review: Possible strategies for the control and stabilization of Marangoni flow in laterally heated floating zones. *FDMP: Fluid Dynamics & Materials Processing*, vol. 1, no. 2, pp. 171 – 188.

Leypoldt, J.; Kuhlmann, H. C.; Rath, H. J. (2000): Three-dimensional numerical simulations of thermocapillary flows in cylindrical liquid bridges. *J. Fluid Mech.*, vol. 414, pp. 285 – 314.

Melnikov, D. E.; Shevtsova, V. M.; Legros, J. C. (2004): Onset of temporal aperiodicity in high Prandtl number liquid bridge under terrestrial conditions. *Phys. Fluids*, vol. 16, pp. 1746 – 1757.

Melnikov, D. E.; Shevtsova, V. M.; Legros, J. C. (2005): Route to aperiodicity followed by high Prandtl number liquid bridge. 1-g case. *Acta Astronautica*, vol. 56, pp. 601 – 611.

Muehlner, K. A.; Schatz, M.; Petrov, V.; McCormic, W. D.; Swift, J. B.; Swinney, H. L. (1997): Observation of helical traveling-wave convection in a liquid bridge. *Phys. Fluids*, vol. 9, pp. 1850 – 1852.

Preisser, F.; Schwabe, D.; Scharmann, A. (1983): Steady and oscillatory thermocapillary convection in liquid columns with free cylindrical surface. *J. Fluid Mech.*, vol. 126, pp. 545 – 567.

Schwabe, D. (2005): Hydrodynamic instabilities under microgravity in a differentially heated long liquid bridge with aspect ratio near the Rayleigh-limit: Experimental results. *Advances in Space Research*, pp. 36 – 42.

Shevtsova, V. M.; Melnikov, D. E.; Legros, J. C. (2001): Three-dimensional simulations of hydrodynamical instability in liquid bridges. Influence of temperature-dependent viscosity. *Phys. Fluids*, vol. 13, pp. 2851 – 2865.

Shevtsova, V. M.; Melnikov, D. E.; Legros, J. C. (2003): Multistability of the oscillatory thermocapillary convection in liquid bridge. *Phys. Rev. E*, vol. 68, pp. 066311.

Shevtsova, V. M.; Mojahed, M.; Legros, J. C. (1999): The loss of stability in ground based experiments in liquid bridges. *Acta Astronautica*, vol. 44, pp. 625 – 634.

Shevtsova, V. M.; Mojahed, M.; Melnikov, D. E.; Legros, J. C. (2003): The choice of the critical mode of hydrothermal instability by liquid bridges. *Lecture Notes in Physics "Interfacial Fluid Dynamics and Transport Processes"*, vol. 628, pp. 240 – 262.

Velten, R.; Schwabe, D.; Scharmann, A. (1991): The periodic instabiiity of themocapillary convection in cylindricai liquid bridges. *Phys. Fluids A*, vol. 3, pp. 267 – 279.

Wanschura, M.; Shevtsova, V. M.; Kuhlmann, H. C.; Rath, H. J. (1995): Convective instability mechanisms in thermocapillary liquid bridges. *Phys. Fluids*, vol. 5, pp. 912 – 925.

Xu, J.-J.; Davis, S. H. (1984): Convective thermocapillary instabilities in liquid bridges. *Phys. Fluids*, vol. 27, pp. 1102 – 1107.